International Journal of Applied Pharmaceutics

ISSN- 0975-7058 Vol 18, Issue 2, 2026

Original Article

FORMULATION, CHARACTERIZATION AND PHARMACOKINETIC EVALUATION OF RIVAROXABAN-CITRIC ACID COCRYSTALS WITH ENHANCED SOLUBILITY, STABILITY AND BIOAVAILABILITY

DEEPAK KULKARNI[1*], SANJAY PEKAMWAR[1], PRASHANT TANDALE[2]

[1]School of Pharmacy SRTM University, Nanded-431606, Maharashtra, India. [2]Department of Pharmaceutical Sciences, Lovely Professional University, Punjab, India

*Corresponding author: Deepak Kulkarni; *Email: deepakkulkarni68@gail.com

Received: 16 Nov 2025, Revised and Accepted: 29 Dec 2025

ABSTRACT

Objective: The attempt was made to improve solubility, flow properties, stability and bioavailability of rivaroxaban (RRB) by cocrystal formation.

Methods: The attempt was made to fabricate microwave assisted cocrystals of RRB using 10 different solid carboxylic acids as a cocrystal formers in 1:1 and 1:2 stoichiometric ratio. All the drug-coformer combinations were subjected to solubility analysis. Rivaroxaban-citric acid (RRB-CA)was further subjected to characterizations like Fourier transform infrared (FTIR), differential scanning colorimetry (DSC) and x-ray diffraction (XRD) to confirm the formation cocrystals as it shown highest solubility sediment delivery model (SeDeM) analysis was implemented to estimate comparative compressibility of pure drug and cocrystals. Cocrystals were further formulated into an immediate-release tablet and subjected to dissolution analysis in comparison with pure drug tablet. The comparative pharmacokinetic analysis was performed using *wistar rats* to. The comparative stability and shelf-life analysis was performed.

Results: Solubility analysis showed highest solubility with RRB-CA combination. The characterizations like FTIR, DSC and XRD confirmed the formation cocrystals. SeDeM (Sediment Delivery Model) analysis showed improved flowability and compressibility after cocrystal formation. The comparative dissolution study performed with pure RRB tablet and RRB-CA cocrystals showed improved dissolution after cocrystallizaion. The pure drug showed % drug release60.02±3.80% while RRB-CA cocrystals showed the drug release of 99.20±2.89%. Pharmacokinetic analysis performed using *wistar rats* demonstrated the improved bioavailability of RRB when administered as cocrystal. The pharmacokinetic parameters like peak plasma concentration (Cmax), AUC_{0-t}(area under curve 0-t) and $AUC_{0-\infty}$(area under curve 0-∞)were significantly improved with cocrystallization. The peak plasma concentration of RRB pure drug was14.3389±1.4116µg/ml while for RRB-CA cocrystal it was 23.9644±1.5870 µg/ml. In shelf-life analysis, RRB showed the shelf life of 15.45 mo while cocrystal tablet showed the shelf life of 26.25 mo.

Conclusion: The cocrystallization of RRB with CA resulted in improved solubility by 5.80 folds while powdered dissolution showed the improvement by 1.65 folds. The results of kinetic study also demonstrated the improvement Cmax by 1.67 folds and AUC by 1.55 folds. Overall, the cocrystallization resulted in improved solubility, dissolution, bioavailability and stability.

Keywords: Rivaroxaban, Citric acid, Cocrystals, Solubility, Dissolution, Bioavailability

© 2026 The Authors. Published by Innovare Academic Sciences Pvt Ltd. This is an open access article under the CC BY license (https://creativecommons.org/licenses/by/4.0/)
DOI: https://dx.doi.org/10.22159/ijap.2026v18i2.57537 Journal homepage: https://innovareacademics.in/journals/index.php/ijap

INTRODUCTION

RRB is a novel oral anticoagulant that shows a competitive inhibitory effect on factor Xa. It is as efficient in inhibiting clot-bound factor Xa as it is for unbound factor Xa. It is an oxazolidinone derivative prominent for treating deep vein thrombosis, as it prevents the formation of thombin due to cessation of the coagulation chain reaction [1]. Half-life ranges between 5-9 h, which can be prolonged to 11-13 h in older patients. Even with these properties, RRB belongs to class II of the biopharmaceutical classification system (BCS) system, having low solubility and high permeability. It is slightly soluble in the aqueous medium, showing 5-7 mg/l. The limited and pH-independent solubility of RRB affects the oral bioavailability, which not only intricate the formulation but also lowers patient compliance due to repeated dosing [2]. Limited solubility of the RRB not only affects the plasma concentration but also has a major impact on the dissolution rate, leading to improper formulation response. It has been a problem for formulation scientists ever since.

Researchers have explored many techniques that may increase the solubility, such as physical tempering and chemical modifications. Techniques like nanonisation, micronisation, solid dispersions, complexation, salt formation and cocrystallization are extensively explored [3]. These listed techniques are capable of reducing the particle size or increasing the wettability of the produced particles, but the problems during the formulation of final dosage forms are not taken into account by these methods. Issues like flow property, cohesive interactions, and stability of the drug are what make the final formulation fail in performance standards. These difficulties can be amended by employing cocrystallization as a solubility enhancement strategy [4]. Crystal engineering and crystallisation came into being more than 60 years ago. In 1989, Desiraju defined it as a field of understanding the intermolecular interaction inside crystal packing and utilising it for the formation of new systems with desired physicochemical properties [5].

Cocrystallization is the technique of compounding a multicomponent system called cocrystals. FDA states them as a multicomponent system made up of a drug and a coformer of choice, both interlocked with some interactive forces in an equimolar ratio [6]. Intermolecular interactions such as van der Waals forces, hydrogen bonding, π-π bonding and sometimes ionic bonding.

There are many methods listed in the literature that can be used to formulate the cocrystals. Methods like dry and solvent-aided grinding, slurry crystallisation, solvent evaporation, ultrasonication, hot melt extrusion technique, reactive cocrystallisation, anti-solvent method and many more [6, 7].

Dry grinding, also known as neat grinding, is a technique of grinding a coformer and drug together in a stoichiometric ratio in a mortar pestle or a ball mill. It is a simple and less time-consuming technique, but issues with the generation of amorphous material during grinding and incomplete crystal formation may also arise with this type of produced cocrystals [8]. Analogous to this, solvent-aided grinding is another technique in which similar steps are followed, but in the presence of a suitable solvent. The solvent works

as a catalyst, which eases the molecular interaction, and makes it a simple and easy technique to form polymorphic crystals, but the drawback is the scalability of the method [9].

Slurry crystallisation also uses the solvent to make a suspension/slurry of a mix of drug and cocrystal former. The formed slurry is then either evaporated or dried, and the remnant powder forms the formed cocrystals. It makes thermodynamically stable cocrystals using natural solvents, making it a green synthesis technique for cocrystallisation, but a risk of imperfect crystal formation also follows this technique, and the selection of a solvent in which both the components are soluble is also a distinguishing criterion, making it more tedious [10].

A less frequently used method is cooling crystallisation, in which the coformers and drug are added to a solvent at high temperatures. At increased temperature, a greater quantity is solubilised in the solvent, which, when later cooled, transits into a supersaturated solution, yielding the cocrystals. It is a convenient method at a laboratory scale, but not suitable for drugs and coformers that are thermally unstable [11].

The ultrasonication or sonication aided cocrystallisation technique uses the principles of ultrasonic waves, which are passed through a solution in which the drug and coformer are mixed. The passed waves help to enhance the nucleation, leading to much smaller and homogenous crystal size, but scalability and formation of unstable polymorphic form are major drawbacks of this process [12, 13].

Solvent evaporation is one of the most employed techniques for cocrystal formulation. This process can be combined with a microwave, which makes it faster and more feasible, and leads to the formation of cocrystals with controlled size. It has risen as an efficient, scalable and rapid technique. During the formulation of cocrystals using this method, the solvent is selected that can be easily evaporated, and the drug and coformers are added to it at an equimolar ratio. The formed solution of drug-coformer is then placed in a microwave system though which microwaves are passed. As the microwaves are passed two consequences follows, one in which the passing of microwaves produces dielectric heating as the molecules are lined up and misaligned according to passed waves, leading to evaporation of solvent making it supersaturated and second in which the microwaves are carrying intense energy that fractures the existing molecules, and gives chance to formation of new multicomponent systems with non-covalent intermolecular attractive forces. It is a rapid and easily scalable process as it uses less amount of solvents, making it a sustainable and green process [14, 15]. To overcome the solubility and bioavailability limitations of RRB the cocrystals were fabricated by microwave synthesizer-assisted solvent evaporation using solid carboxylic acids as a cocrystal formers in 1:1 and 1:2 stochiometric ratio. The drug-coformer combination with highest solubility was further subjected to various characterizations like FTIR DSC, and XRD to confirm the cocrystal formation. The dissolution study was performed to demonstrate the improved drug release and pharmacokinetic analysis was performed to demonstrate improved bioavailability. Solubility enhancement RRB remained a challenge due to unavailability of scalable and pharmaceutically acceptable technique. The technique we implemented in study, i.e., microwave-assisted solvent evaporation using ethanol is green and safe approach. The methodology is scalable and pharmaceutically acceptable with high level of precision. The SeDeM analysis reveals the good compressibility for tabletting. Shelf-life improvement indicates improved stability. Such kind of multifaceted advantages were lacking in former studies. We hypothesized that cocrystallization of RRB with CA, a coformer not previously explored for this drug, would create a stable heterosynthon leading to significant improvements in solubility, bioavailability, and tablet ability, thereby addressing multiple limitations of RRB simultaneously.

MATERIALS AND METHODS

Rivaroxaban (99% purity) was received as a gift sample from RV Life sciences, Chhatrapati Sambhajinagar. All the solid carboxylic acids (analytical grade) and tablet excipients (pharmaceutical grade) were procured from Deepalaboratory Chemicals (DLC), Chhatrapati Sambhajinagar. Ethanol (analytical grade) was procured from Sugar Factory, Kopargaon.

Methods

Formulation of cocrystals

The approach selected for the fabrication of co-crystals greatly affects their structural characteristics, particle size, dispersity, and purity. Novel RRB cocrystals were synthesized utilizing a microwave synthesizer-assisted solvent evaporation technique, and 10 cocrystal formers were used in a 1:1 and 1:2 stoichiometric ratio for the preparation of cocrystals. The cocrystal formers were primary selected on the basis of safety and suitability for oral administration. Furthermore, the hydrogen bond formation ability of cocrystal former is important criteria to be considered for the formation of homo and heterosynthons for solubility enhancement. The 1:1 and 1:2 stoichiometric ratio were selected due to balanced availability of hydrogen bond donors and acceptors between drug and cocrystal formers. Higher stoichiometric ratios may result in salt formation or non-distinct cocrystal phases like physical mixtures. The drug (RRB, 435.9 mg) and cocrystal former (respective molecular weight) were dissolved in 10 mlethanol and further evaporated using a microwave synthesizer at 85 watt for maximum 10 min (5 cycles of 2 min each) until complete evaporation of solvent. The resulting cocrystals were subjected to preliminary characterization [16, 17].

Solubility analysis of cocrystals

RRB and prepared cocrystals underwent saturation solubility analysis. Both were added to a volumetric flask containing 10 ml of distilled water and kept on a rotary shaker for 24 h. The solutions were filtered through whatman filter paper (grade 42 and pore size 2.5 µm) at 25.0±0.5 °C and the filtrate was analyzed though a UV spectrophotometer for soluble concentration [18].

Partition coefficient analysis

The cocrystals with highest solubility were subjected to partition coefficient determination. Shake flask method was used for comparative determination of partition coefficient of pure RRB and cocrystals in octanol-water system. 10 mg pure RRB and RRB-CA cocrystals were added in two different vials containing 5 ml water and 5 ml octanol. Both the vials were subjected to shaking for 24 h. Water-octanol layer shows separation. From water and octanol portion 1 ml sample was collected and subjected to UV spectrophotometric analysis after optimum dilution. Partition coefficient was calculated from the ratio of concentration of drug in octanol and water. This value was further subjected to logarithmic conversion to calculate log P [19].

Characterization of cocrystals

Further characterization of RRB, coformers, and cocrystals possessing the highest solubility was subjected to analysis like FTIR, DCS, and XRD to confirm the formation of cocrystals.

FTIR analysis

Formation of a new molecular phase can be confirmed by studying the intermolecular interactions between cocrystals and parent materials. FTIR analysis was performed for RRB, CA and RRB-CA cocrystals. An At FTIR (Agilent, Cary 630, Germany) was employed to study the intermolecular interaction present in pure drug, selected coformer, and prepared cocrystals. The IR absorption spectra were obtained in the range of 4000 to 400 cm^{-1}. The obtained data were then compared to study the interactivity between RRB and CA [20].

Differential scanning calorimetry

DSC is an extensively used technique to study compatibility and thermal behavior of the drug, cocrystal former and prepared cocrystals. Thermal analysis of RRB, CA, and RRB-CA was done using a DSC-60 (Mettler Toledo, Switzerland). Aluminium powder was used as a reference, and aluminium cells served as a sample holder during analysis. About 4-5 mg of the sample was placed in a sample cell and heated from RT to 300 °C with a heating rate was maintained at 5 °C/min, in an inert nitrogen atmosphere to prevent oxidative reactions [21].

X ray diffraction

Diffraction patterns for RRB, CA, and RRB-CA cocrystals were obtained using the (Bruker D2 Phaser, Germany) diffractometer; the angular range was set to 5 to 50°, and a voltage and current of 40kV and 55mA were used, respectively. Scan rate was about 0.05°/sec, and each step was about 180 seconds [22].

Flow property and SeDeM analysis

When various single components are compounded as a polymorph, the originated substance differs in flowing characteristics. To assess this change flow properties of cocrystals can be compared to the original drug. Herein, bulk and tapped density, along with Carr's index, Hausner's ratio and angle of repose of RRB and RRB-CA cocrystals were compared. The goal was to determine whether there is any enhancement in the flow characteristics of powder post-cocrystallization. SeDeM analysis was performed on the basis of various parameters like dimension, compressibility, flowability and lubricity. The experimental values were converted into radii value using conversion factor for particular parameter. From the radii (r) value profile parameter index (IPP) and good compressibility index (IGC) were calculated using following formulas. The SeDeM diagram was created by plotting radar plot on the basis of r value[23].

$$IPP = \text{Average r of all parameters} \quad \text{Eq. 1}$$

$$IGC = IPP \times f \quad \text{Eq. 2}$$

where f is reliability factor calculated from polygon area and circle area in the radar plot and for 12 parameters the standard value is 0.952 [24].

Powder dissolution study

USP II type apparatus, also known as a rotating paddle apparatus, consisting phosphate buffer system of pH 6.8 as dissolution media was used. RRB, as a pure drug and formed cocrystals, were tested for dissolution, and their comparative drug release was analyzed using a UV spectrophotometer [25].

Formulation and optimization of a tablet

Upon crystallization, the improvement in dissolution characteristics was determined comparatively between RRB and its cocrystals with CA. An immediate-release tablet was formulated and optimized using a 2^2factorial design. Drug release was considered as a response (dependent variable) to the independent variables like binder (sodium starch glycolate/SSG) and lubricant (magnesium stearate/MS) concentration. The software used for this process is Design Expert 13 (trial version), binder, and lubricant concentration were considered as X1 and X2, respectively. The table 1 elucidates the coded as well as actual values for the independent variables [26].

As shown in the coded and actual value table above total of 4 runs were recommended. 4 tablet batches were formulated as suggested by design expert and illustrated in table 2.

Table 1: Suggested experimental runs with coded value and actual values

Formulation code	Variables level [Coded values]		Variables level [Actual values]	
	X1	X2	X1	X2
F1	-1	-1	4	1.5
F2	-1	+1	4	3
F3	+1	-1	6	1.5
F4	+1	+1	6	3

X1: Binder (Sodium Starch Glycolate) concentration (mg); X2: Lubricant (Magnesium Stearate) concentration (mg). Different concentrations of independent variables were shown by X1 being the highest level, while X2 being the lowest level.

Table 2: Experimental runs consisting of actual values of all materials

S. No.	Ingredients (mg)	Batch code				
		F1	F2	F3	F4	Pure RRB tablet
1	Rivaroxaban cocrystals*	28.81	28.81	28.81	28.81	20
2	Lactose monohydrate	85	85	85	85	85
3	MCC PH_{102}	58.69	57.19	56.69	55.19	67.5
4	Starch	20	20	20	20	20
5	Sodium starch glycolate	4	4	6	6	4
6	Talc	1	1	1	1	1
7	Sodium lauryl sulphate	1	1	1	1	1
8	Magnesium stearate	1.5	3	1.5	3	1.5
	Total (mg)	200	200	200	200	200

*Amount equivalent to 20 mg of Rivaroxaban

Characterization of tablet blend

The characterization involved testing the tablet blend for bulk and tapped density, Carr's index, Hausner's ratio and angle of repose. Upon preformulation testing, tablets were compressed and tested for hardness, thickness, weight variability and friability [27].

Dissolution study of tablet

Tablets of RRB-CA cocrystals were successfully formulated and were subjected to tests for dissolution in contrast to tablets of pure RRB. The same process parameters of optimized batch of RRB-CA tablet were used to prepare pure RRB tablets. The dissolution was carried out using a phosphate buffer with 6.8 pH at a maintained temperature of 37±0.5 °C. At a predetermined rate, samples were collected and assessed though a UV spectrophotometer for enhancement in drug release from the RRB-CA cocrystal tablet [28].

Pharmacokinetic study

The protocol for pharmacokinetics was approved by institutional animal ethical committee (IAEC) of Invitox R and D institute with approval no. IRDI/IAEC/T-01/2024-25 dated 02/02/2025. The study aimed to compare the oral bioavailability of pure RRB and its crystal with CA using *wistar rats.* Eight animals were randomly divided into two groups; one group received pure drug powder, while the second was administered with cocrystal powder. Animals were fasted overnight with free access to water before administration. Pure RRB and RRB-CA cocrystals were orally administered at a dose of 2.06 mg/kg, followed by the collection of blood samples from the retro-orbital plexus. Sampling was done in triplicate from every animal, at pre-determined intervals of 0.5, 1, 3, 6, 12, 24, 36, and 48 h. The sampled blood was then transferred into a polypropylene bag containing the solution of disodium salt of EDTA (ethylene diamine tetra acetic acid) (anti-coagulant). Liquid-liquid extraction method was utilized for the isolation of pure RRB and RRB-CA cocrystals, and the isolate was then vortexed for 10 min, followed by centrifugation at 4000 rpm and stored at-20 °C. For further analysis, supernatants from each sample were collected in tubes and evaporated at 40 °C to reach complete dryness. 500 µl of Acetonitrile was added to tubes containing the dried sample and vortexed before adding them to vials for injection [29].

Plasma concentration of animals following oral administration of pure RRB and RRB-CA cocrystals was analyzed using non-compartmental models in PKSolver (version 2.0) pharmacokinetic software.

Stability study and shelf-life analysis

Accelerated stability study was performed at 40±2 °C and 75±5% RH in desiccator. Various evaluation parameters like hardness, drug content and dissolution were determined after the period of three months to assess the stability of pure drug and cocrystal tablet. Shelf-life was estimated from degradation data at accelerated conditions assuming first order kinetics and extrapolating to 90% of initial drug content [30].

RESULTS AND DISCUSSION

Solubility analysis

Solubility analysis was performed for pure drug RRB and various cocrystals prepared with multiple cocrystal formers. The melting point and solubility of RRB and its cocrystals was analyzed in distilled water and illustrated in table 3 [31].

Table 3: Saturation solubility and melting point analysis

Drug/Coformer	Melting point coformer	Cocrystal melting point [1:1]	Solubility [mg/ml][1:1]	Cocrystal melting point [1:2]	Solubility [mg/ml][1:2]
Rivaroxaban [RRB]	229-232	-	0.1006±0.0101	-	-
RRB+Citric acid	149-151	151-154	0.5838±0.0291	181-183	0.2911±0.0286
RRB+Tartaric acid	162-165	189-192	0.1431±0.0149	191-194	0.1375±0.0121
RRB+Salicylic acid	151-153	176-178	0.1297±0.0125	182-184	0.1189±0.0142
RRB+Oxalic acid	174-179	191-194	0.2139±0.0186	180-182	0.2234±0.0263
RRB+Ascorbic acid	171-173	188-191	0.2367±0.0320	185-188	0.2421±0.0219
RRB+Acetyl salicylic acid	141-143	171-173	0.1417±0.0358	177-179	0.1217±0.0213
RRB+Maleic acid	131-134	167-170	0.1520±0.0162	172-174	0.1339±0.0255
RRB+Anthranillic acid	144-148	221-224	0.1724±0.0410	214-219	0.1826±0.0397
RRB+Benzoic acid	117-119	156-158	0.1694±0.0326	159-163	0.1589±0.0243
RRB+Sulpho benzoic acid	114-117	149-153	0.1742±0.0307	155-157	0.1572±0.0259

SD±n = 3. Solubility determined in distilled water at 25 °C after 24 h. The 1:1 RRB–CA cocrystal showed a 5.8-fold solubility enhancement over pure RRB.

The pure RRB showed melting in the range of 229-232 °C and was solubilized at a concentration of 0.1006±0.0101 mg/ml. Cocrystallization of RRB showed enhancement in solubility characteristics of all prepared cocrystals, but an outstanding increase was seen in the RRB-CA cocrystals, with solubility of 0.5838±0.0291 and 0.2911±0.0286for 1:1 and 1:2, respectively. RRB-CA cocrystals in a 1:1 ratio exhibited a 5.8-fold increase; meanwhile, 1:2 ratio showed a 2.89-fold increase. This increment insolubility is the result of weak hydrogen bonding interaction result in formation of heterosynthon between RRB and CA. The structures of all cocrystal formers and possible hydrogen bonding interactions between RRB and CA are illustrated in fig. 1a and b [32, 33].

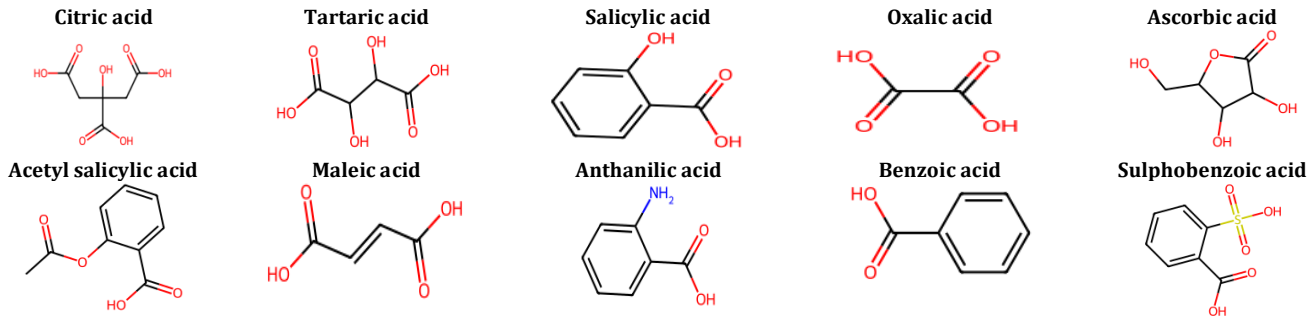

Fig. 1a: Structures of solid carboxylic acids used as cocrystal formers (CCF)

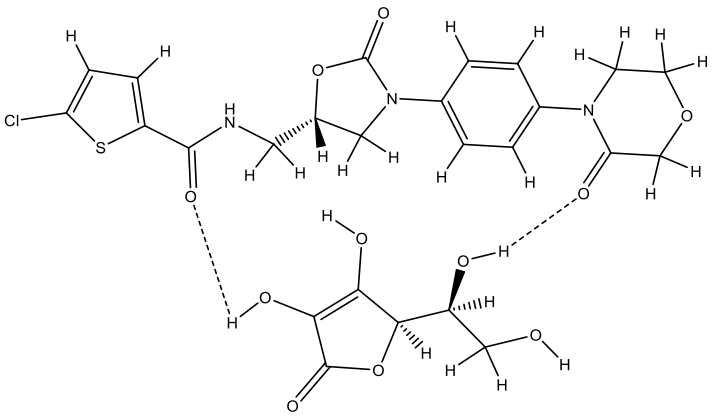

Fig. 1b: Possible hydrogen bond formation between RRB-CA

The extent of the solubility enhancement was notably high for RRB-CA cocrystals, followed by RRB-Ascorbic acid cocrystals in a 1:2 and 1:1 ratio, then RRB-Oxalic acid cocrystals, having 0.2421±0.0219 mg/ml, 0.2367±0.0320 mg/ml, and 0.2234±0.0263 mg/mlconcentration. The crystallization of RRB with other cocrystal formers like benzoic and sulphobenzoic acid, maleic acid, anthranillic acid, salicylic and acetyl salicylic acid showed an insignificant effect on solubility. Shifts in the melting point to the lower temperatures also confirmed the successful formation of cocrystals. Among the various coformers screened, citric acid proved most effective in enhancing the solubility of the drug due to its unique structural and chemical characteristics. It possesses three carboxylic acid and one hydroxyl group, allowing extensive hydrogen bonding with the amide and carbonyl groups of the drug, leading to a more hydrophilic and less tightly packed crystal lattice. The high polarity and water solubility of citric acid facilitate improved wetting and dissolution of the cocrystal [33, 34].

Partition coefficient analysis

Determination partition coefficient is one of the important analyses to demonstrate the improved solubility. Partition coefficient (octanol/water) was found to be decreased after cocrystallization. The log P value of pure RRB was found to be 1.60±0.16, while RRB-CA cocrystal showed log P value of 1.34±0.11. The decrease in log P value indicates increase in partition of RRB in water is due to improved water solubility after cocrystllization with CA [35].

FTIR analysis

Alteration in the structure of newly formed cocrystals studied comparatively with parent materials. The fig. 2 presents the FTIR spectra of pure RRB, cocrystal former CA and RRB-CA cocrystals.

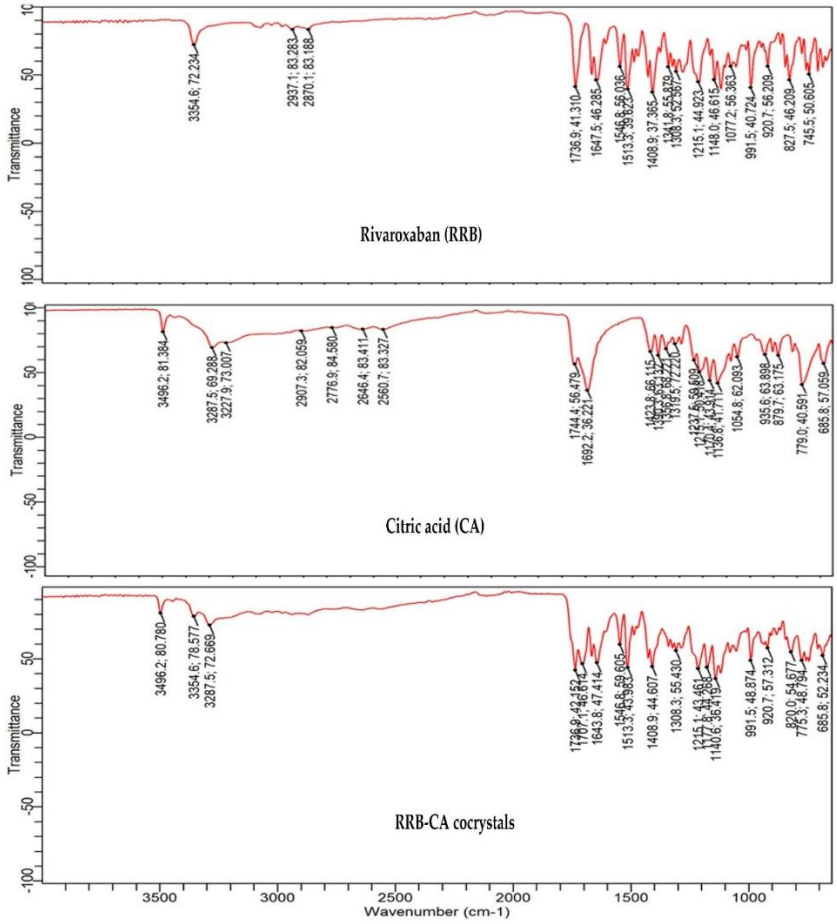

Fig. 2: FTIR spectra of RRB, CA and RRB-CA cocrystals

The obtained spectrum aids in the interaction study between RRB and RRB-CA cocrystals. The spectrum of pure RRB indicates the N-H stretching as the broad absorption can be seen at 3354.6 cm^{-1}. The peaks at 2937.1 cm^{-1} and 2870.1 $cm^{-1}$are due to C-H aliphatic stretching. C=O stretching in ester and amide can be observed at 1736.4 cm^{-1} and 1677.5 cm^{-1}, respectively. Stretching due to the presence of the C-Cl bond can be seen in the region of 850-550 cm^{-1}. C-O-C movement was observed at peaks present in the region of 1200-1150 cm^{-1}[36].

For CA coformer peaks obtained at 3496.2 cm^{-1}, 3287.5 cm^{-1}, and 3227.9 cm^{-1} are due to O-H stretching, these peaks often show a broad nature due to strong hydrogen interaction, as hydroxyl and carboxylic acid groups are present. A broad shoulder-like peak can also be seen at 1744.4 cm^{-1} and 1692.6 cm^{-1} as carboxyl groups overlap with the O-H band. The presence of multiple strong peaks in the region of 1300-1000 cm^{-1} indicates the polycarboxylic nature of CA, as they are due to C-O and O-H vibrations. Another two distinctive peaks at 935.6 cm^{-1} and 879.7 cm^{-1} depict the bending of the O-H bond [37].

When the spectra of the formed cocrystal are compared with the two previous spectra, a slight downshift can be observed at 3496.2 cm^{-1} and 3354.6 cm^{-1}. This can be attributed to the hydrogen interaction among the O-H group from the carboxylic acid and the carbonyl N-H of RRB. Another two distinctive peaks at 1707.1 cm^{-1} and 1643.8 cm^{-1} are due to new H-bond formation as a consequence of carbonyl and amide interactions between RRB and CA. These shifts are evident to suggest the formation of a new multicomponent system, along with it vanishing of certain peaks and the arrival of new ones also advocate for cocrystal formation.

DSC analysis

The solid-state properties and thermal behavior of RRB, CA, and RRB-CA were studied in DSC. The procured thermograms show their thermal behavior. The pure RRB gave a sharp endothermic peak with an onset being at 234.06 °C and its peak at 234.93 °C; the high melting point suggests the low solubility of the parent drug molecule. Similarly, for CA onset and peak were observed at 157.38 °C and 160.78 °C, respectively. The formed cocrystals of RRB and CA were distinguished by the origin of a new endothermic event at the onset of 136.59 °C and the peak being 141.36 °C. The comparison of DSC spectra shows possibility of eutectics, but there are many points endorse the formation of cocrystals. XRD pattern shows appearance of new peaks and not superimposed peaks of parent drug and conformer which is a clear indication of new crystalline phase. In DSC of eutectics, multiple endotherms (drug, conformer and eutectic melting) but in case of this study the cocrystal shows sharp and distinct melting point indicating formation of new crystalline phase. When the endothermic peak of the cocrystal and pure RRB were compared, DSC showed a 1.66-fold decrease in the melting point, which describes the enhancement of solubility due to cocrystallization. This significant downward shift in melting onset and peak also marks the formation of a new multicomponent phase. DSC thermograms for RRB, CA and their cocrystals are illustrated in fig. 3 (a, b, c) [38, 39].

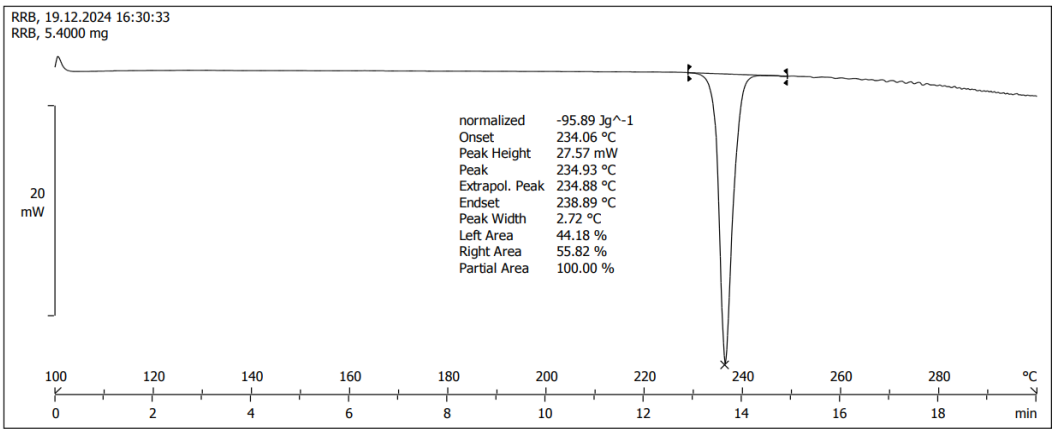

Fig. 3a: DSC thermogram of RRB

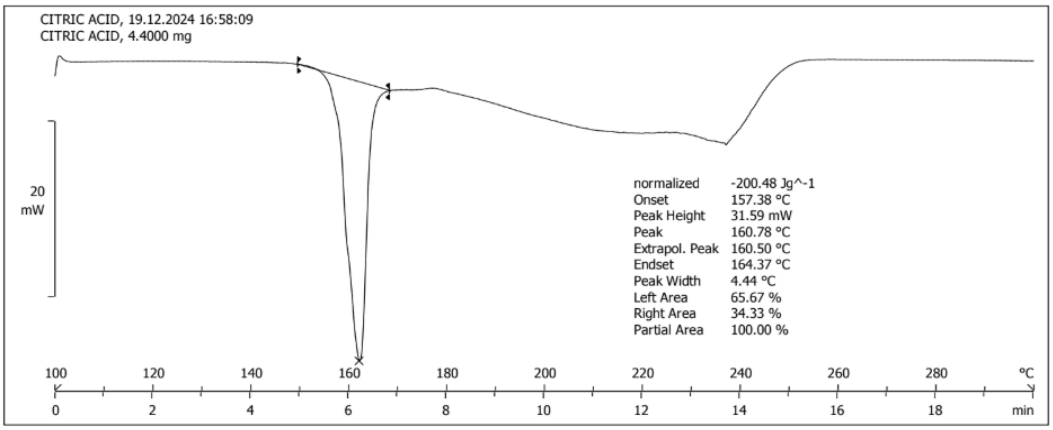

Fig. 3b: DSC thermogram of CA

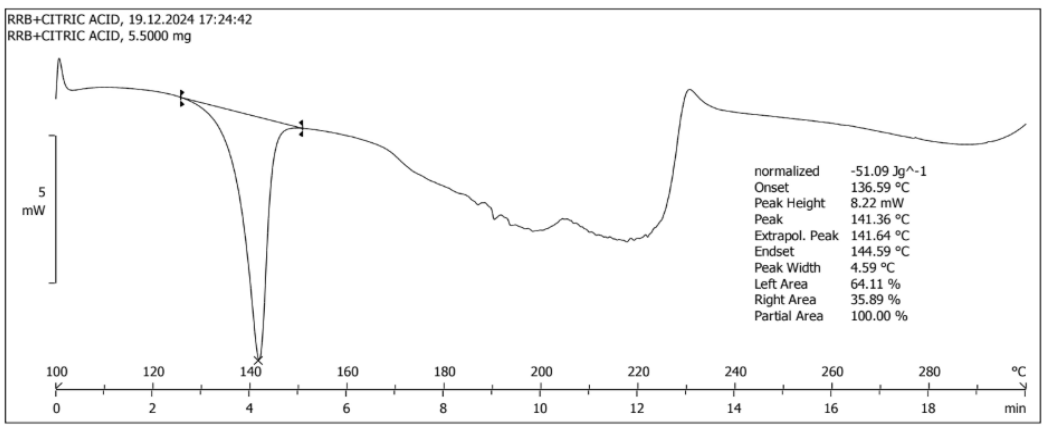

Fig. 3c: DSC thermogram of the RRB–CA cocrystal showing a single, sharp endothermic peak at 141.36 °C, indicative of a new solid phase

XRD analysis

Multiple characteristics of the drug depend upon the solid-state properties, like crystallinity and amorphous nature. The XRD analysis characterizes the drug and formed cocrystals for the degree of their crystallinity. Critical insights were provided by the XRD patterns below regarding the crystalline nature and purity of the samples of RRB, CA and cocrystals (fig. 4a, b, c). The diffractogram obtained of the pure RRB showed distinct 2θ values at 16.528°, 19.929°, 22.49°, 25.644°, and 26.639°, of which the peak at 22.49° was observed to be most intense and followed by peaks at 16.528° and 26.629°. The diffractogram of CA shows the most intense peak at 26.45° and other broader and lesser intensive peaks at 18.626° and 33.832°, indicating the crystallite size is smaller in CA [40, 41].

All the intense and broader peaks observed at different 2θ values do not correspond to new crystals formed. Emergence of this peak at 22.8°, 19.777°, and 18.427° was most intense, reflecting the increased crystallinity. The conclusion derived from this is the synthesis of a well-organized crystal lattice. And the modified properties of the material can be validated though this alteration in the diffractogram of formulated cocrystals.

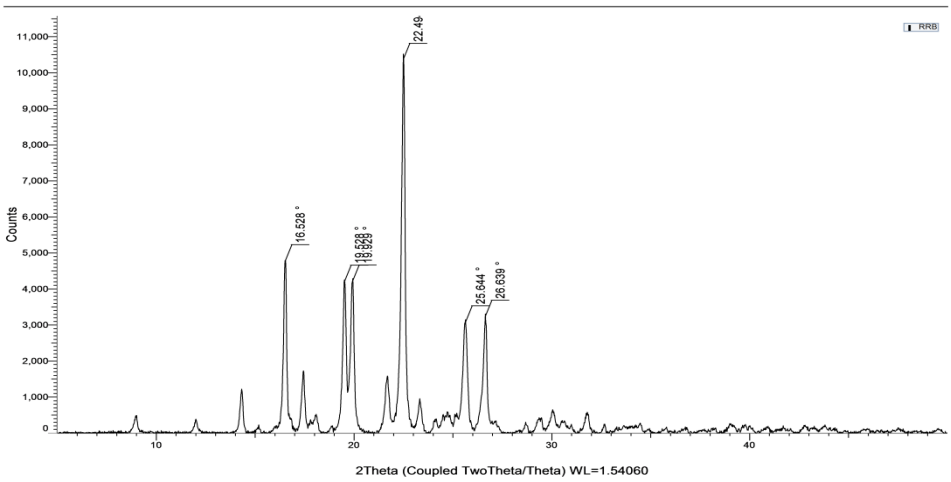

Fig. 4: XRD analysis of RRB

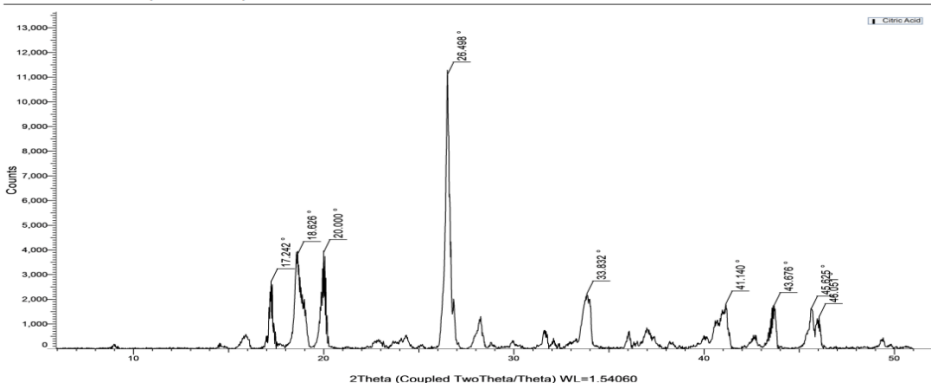

Fig. 4b: XRD analysis of CA

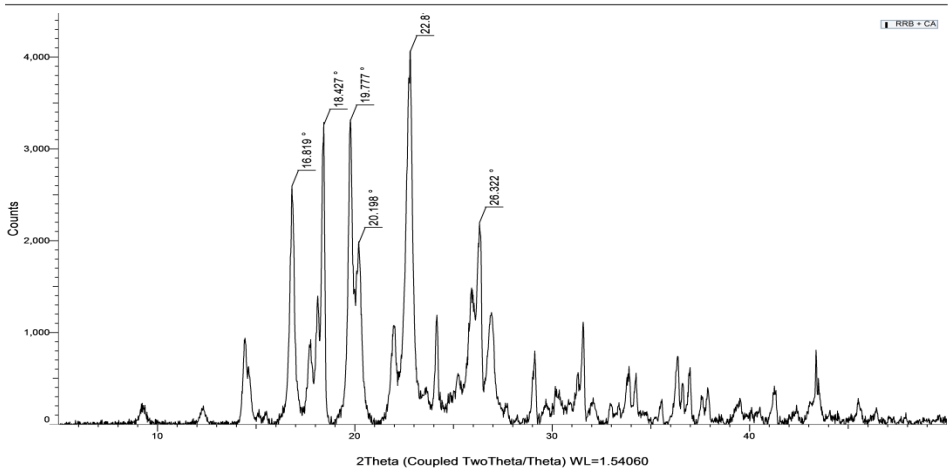

Fig. 4c: PXRD pattern of the RRB–CA cocrystal displaying new characteristic peaks at 2θ = 18.427,19.777 and 26.322, confirming the formation of a distinct crystalline phase different from the parent components

Flow property and SeDeM analysis

From the table given below, it was concluded that there is a significant enhancement in the flow properties of newly formed cocrystals of RRB-CA. This enhancement is mainly attributable to the newly formed particles with varied shapes and sizes than that of the starting materials. Notable decrease in the angle of repose, Hausner's ratio and Carr's index suggests the betterment of flow.

Improvement in this particular property is beneficial for better processing of cocrystals during tableting and capsule-filling, and it also helps in content uniformity of crystals during mixing. Flow properties of RRB and RRB-CA cocrystals are presented in table 4.

Table 4: Flow properties of RRB and RRB-CA cocrystals

Properties	Angle of repose	Bulk density	Tapped density	Carr's index	Hausner's ratio
Rivaroxaban	37.10±1.25	0.42±0.012	0.54±0.020	22.22±0.66	1.28±0.011
RRB-CA Cocrystal	29.92±1.13	0.47±0.019	0.55±0.023	14.54±0.12	1.17±0.002

Data presented as mean±SD (n = 3)

The SeDeM analysis carried out on the basis of various dimensions, compressibility, flowability and lubricity parameters. All the values and their conversion in radii value is well illustrated in table 3.

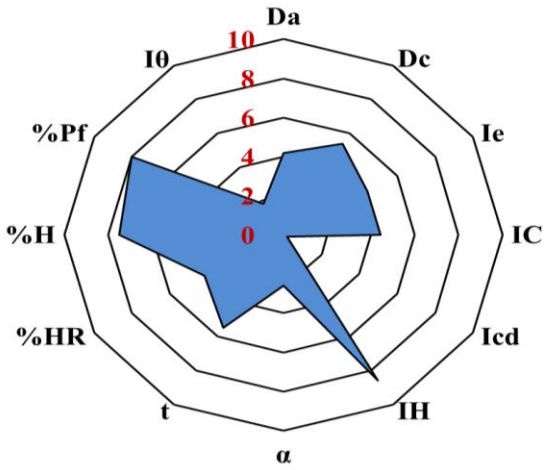

Fig. 5a: SeDeM diagram pure RRB

From the radii (r) value of 12 different parameters included in SeDeManalysis (table 5) a radar plot is created which is also described as SeDeM diagram (fig. 5a and 5b). From SeDeM analysis and diagram two important parameters, namely, IPP and IGC were calculated for both pure RSC and RRB-CA cocrystals. The IPP value for pure RRB was 4.74 and IGC value was 4.51 while IPP value for RRB-CA cocrystals was found to be 5.66 and IGC value was found to be 5.39. The IGC value of more than 5 for RRB-CA cocrystals indicates better compressibility and tabletting efficiency [42].

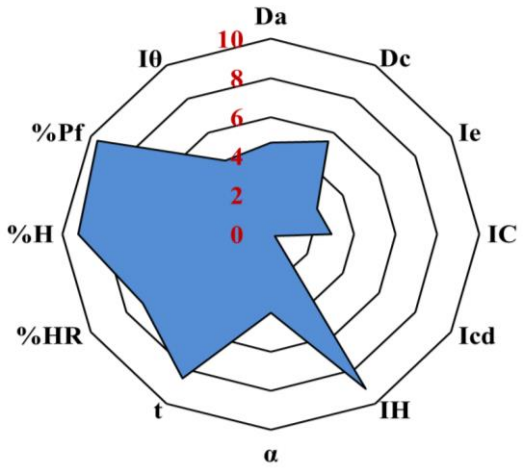

Fig. 5b: SeDeM diagram RRB-CA cocrystals

Table 5: SeDeM analysis parameters for RRB pure drug and RRB-CA cocrystals

Incidence factor	Parameter	Value [v] for pure RRB	Value [v] for RRB-CA cocrystals	Factor	r [value for pure RRB]	Mean incidence [for pure RRB]	r [value for pure RRB-CA cocrystals]	Mean incidence [for pure RRB-CA cocrystals]
Dimension	Bulk Density [Da]	0.42	0.47	10v	4.20	4.8	4.70	
	Tapped Density [Dc]	0.54	0.55	10v	5.40		5.50	5.10
Compressibility	Inter-particle Porosity [Ie]	0.53	0.31	10v/1.2	4.42	3.02	2.58	1.90
	Carr Index [IC]	22.22	14.54	v/5	4.44		2.91	
	Cohesion Index [Icd]	4.0	4.2	v/20	0.20		0.21	
Flowability/Powder Flow	Hausner Ratio [IH]	1.28	1.17	[30-10v]/2	8.60	5.56	9.15	7.22
	Angle of Repose [α]	37.10	29.92	10-[v/5]	2.58		4.016	
	Powder Flow [t]	9	3	10-[v/2]	5.5		8.5	
Lubricity/Stability	Loss on Drying [%H]	5.85	2.89	10-v	4.15	5.83	7.11	8.18
	Hygroscopicity [%H]	4.98	1.47	10-[v/2]	7.51		9.26	
Lubricity/Dosage	Particles<50 µm [%Pf]	10	2	10-[v/5]	8	4.92	9.6	6.975
	Homogeneity Index [Iθ]	0.0037	0.0087	500v	1.85		4.35	
Parameter profile index [IPP]					4.74	-	5.66	-
Good compressibility index [IGC]					4.51		5.39	-

The radius (r) for each parameter was calculated from the experimental value (v) using the specified conversion factor; for Bulk Density (Da): r = 10 × v; for Carr's Index (IC): r = v/5. The parameter profile index (IPP) is the mean of all r values, and the good compressibility index (IGC) = IPP × f, where f is a reliability factor (0.952 for 12 parameters). An IGC>5 indicates good compressibility

Powder dissolution study

When the drug release profile of RRB-CA crystals and pure RRB were compared [fig. 6], it was concluded that the drug release from crystals was substantially greater than that of pure drug. The increase in release rate was observed from the first sampling time point, and it persisted throughout the dissolution process. This enhancement was considered due to low lattice energy, changes in crystal packing, and increased wettability imparted due to the selected conformer [43].

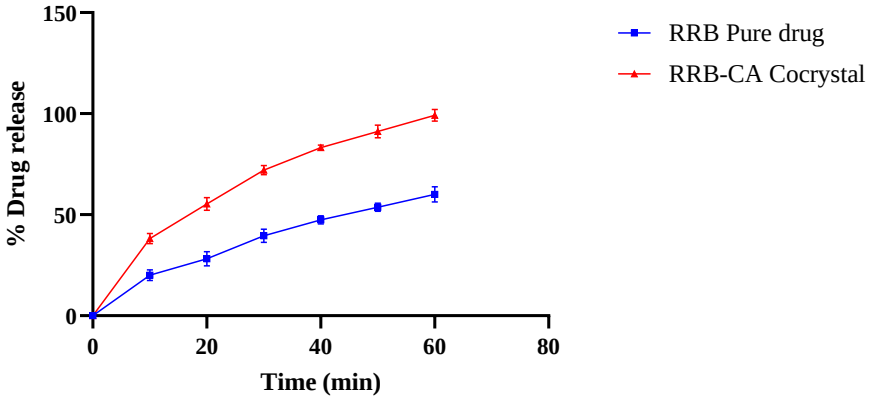

Fig. 6: Powder dissolution study. Error bars indicate SD values, n=3

Evaluation of pre-compression parameters of factorial formulations

The results of the characterization of the tablet blend are illustrated in table 6. From theresults illustrated in table, it was concluded that the blend samples possessed good flow and that they are suitable for compression [44].

Formulation and optimization of tablets

The tablets of the newly formed cocrystals were formulated by employing a two-level, two-factorial experimental design. 2^2experimental design studies the influence of multiple independent variables set at two levels, and also their interactive effect on the response variable. In this study, drug release was considered as a response to the varied concentration of the binder and lubricant at two levels. The tablets of cocrystals were formulated in accordance with the experimental runs provided by the software. Pure drug tablet showed the % drug release of 68.71±2.49 while optimized RRB-CA cocrystal tablet (F1) showed 95.19±2.91 indicating improved dissolution after cocrystallization. The % drug release of RRB from all the tablets is illustrated in fig. 7 [45].

The obtained experimental data were fitted into a selected factorial model with the help of Design Expert software. In the 2^2 factorial design, Factor B (magnesium stearate) showed a statistically significant negative effect ($p = 0.0333$), whereas Factor A (sodium starch glycolate) exhibited a negative but borderline effect ($p = 0.0579$). The overall model was marginally significant ($p = 0.0453$). The results for ANOVA and model fit statistics are given in the table 7a and 7b [46].

Table 6: Table depicting the pre-compression parameters of the factorial formulations

Formulation code	Bulk density [g/cm³]	Tapped density [g/cm³]	Hausner's ratio	Compressibility index [%]	Angle of repose [θ]
F1	0.50±0.019	0.57±0.014	1.14±0.016	12.30±1.18	28.88±1.26
F2	0.51±0.010	0.59±0.023	1.15±0.023	13.52±1.67	29.20±1.21
F3	0.53±0.021	0.61±0.031	1.15±0.013	13.08±0.98	29.76±1.31
F4	0.51±0.017	0.60±0.024	1.17±0.008	14.98±0.57	29.50±1.28
Pure drug RRB tablet	0.44±0.028	0.55±0.031	1.25±0.010	20.02±0.59	36.29±1.16

Results are given in mean±SD, n=3

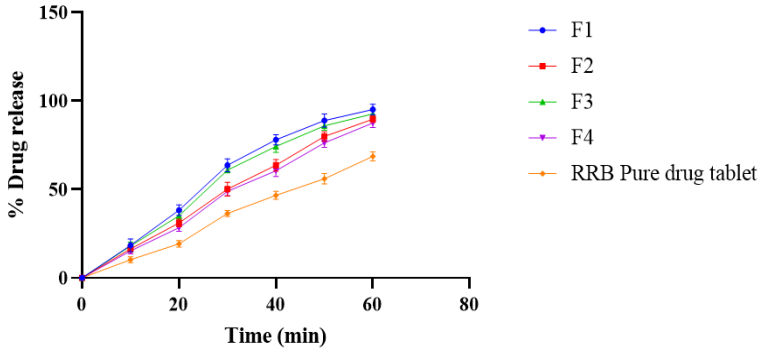

Fig. 7: Comparative dissolution study of experimental tablet batches and pure drug tablet. Error bars indicate SD values, n=3

Table 7a: Table for ANOVA

Source	Sum of squares	df	mean square	F-value	p-value	
Model	31.58	2	15.79	242.81	0.0453	Significant
A-Sodium Starch Glycolate	7.81	1	7.81	120.14	0.0579	
B-Magnesium stearate	23.77	1	23.77	365.48	0.0333	
Residual	0.0650	1	0.0650			
Cor Total	31.64	3				

Table 7b: Table for model fit statistics

Std. Dev.	0.2550	R^2	0.9979
Mean	91.65	Adjusted R^2	0.9938
C. V. %	0.2782	Predicted R^2	0.9671
		Adeq Precision	34.7316

Half normal plot and pareto chart

Multiple graphical tools were also used to specify the adequacy and suitability of the model. The purpose of this half-normal plot was to visually assess the effects of independent variables on the response. Variables examined were SSG and MS; the points that are closer to the y-axis/left side of the plot show a less significant effect on the response. From the half-normal plot, it was concluded that MS has a more dominating negative effect on the drug release; an increase in its concentration reduces the drug release. Correspondingly, increasing the concentration of SSG also shows a negative effect on drug release, but its extent is very much lower compared to MS. Depicted colour coding for both variables shows a negative effect, meaning factors are the limiting factors for the release of the drug from tablets. This summary is very important for the future design of a product. Half normal plot and pareto chart are depicted in fig. 8 [47].

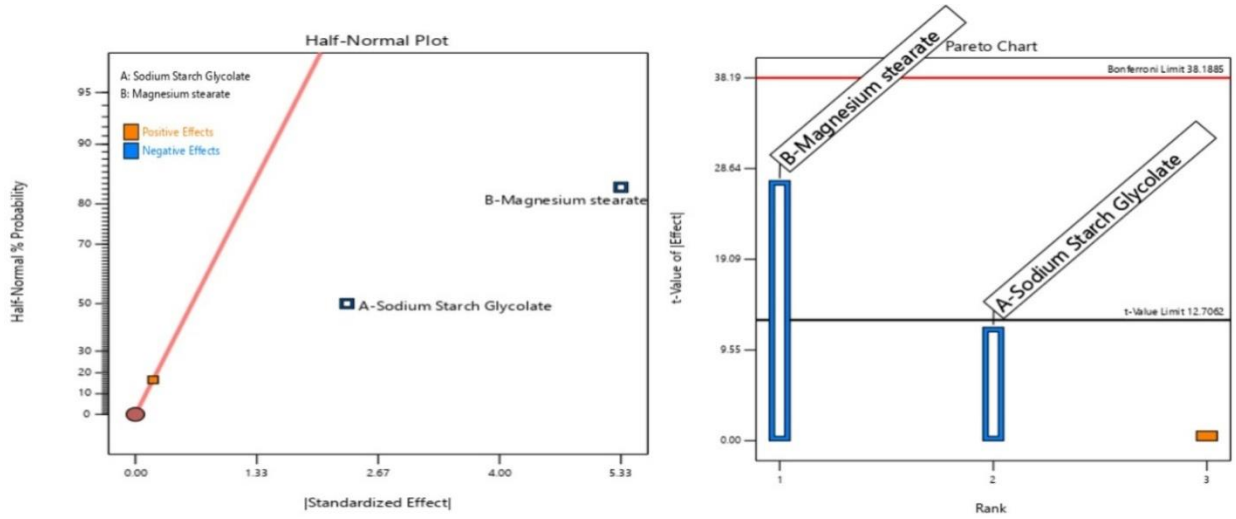

Fig. 8: Half-normal plot and pareto chart to visually assess the effect of variables on drug release from the tablet

A Pareto chart is a tool to further quantify the effects of independent variables on the response shown by a half-normal plot. The chart suggests the most dominant negative effect of MS on the drug release, which can be seen crossing the strict statistical boundaries, like t-value limits. Likewise negative effect was also imparted by SSG, but to a much lesser extent than MS. The effect of SSG does not cross a statistically significant line, adding clarity that it can be further de-emphasized from additional optimization [48].

A perturbation plot is mainly used to study the individual effect of a variable on the response. The actual factors present on the left panel of the plot indicate reference values (centre value for an experiment) for the independent variables, green for SSG being 5 and blue for MS being 2.25. The primary purpose of this plot is to study the effect of deviation of an individual variable, SSG and MS in this case, on response, i. e, % drug release. The decreasing slope after the central point suggests the negative effect of each variable. Meaning increasing the variable concentration above this point retards the % drug release. The sharp decline in the slope of the second variable (MS) indicates a stronger retarding effect on the drug release as compared to the first variable (SSG). Combining the results of the graphical analysis [half-normal plot, Pareto and Perturbation plot], it can be deduced that control over the levels of MS can be prioritized for an increase in % drug release. Perturbation of an interaction plot is illustrated in fig. 9 [49, 50].

The interactions between the independent variables are important to consider during optimization, as the impact of levels of both the independent factors (in this instance, SSG and MS) on the response (% drug release) may be interdependent. The X axis of the plot indicates the concentration of the SSG, and the colored line indicates concentrations of MS (black-1.5 mg and red-3 mg). The interaction effect shows an additive but weak effect (almost parallel lines) of both variables on the % drug release. With the increasing amount of SSG to higher level, % drug release is observed to be decreasing at both concentrations of MS. Likewise change in concentration of MS from low level (1.5 mg) to higher level (3 mg), drug release can be seen decreasing. Altogether, it can be comprehended from this interaction plot that a lower concentration of both variables leads to an increase in % drug release.

Contour plot and 3D RSM analysis

The main purpose of the contour plot is to study the combined impact of the two independent variables herein, SSG and MS, on the % drug

release from the formulated tablet. The colour scale illustrates how changes in the concentrations of both variables can lead to changes in % drug release. From the plot, it can be inferred that the highest drug release (95%) can be obtained at higher concentrations of SSG and lower concentrations of MS. Thus, it can be concluded from the plot that the ideal concentrations can be used to increase the drug release, and this plot serves as a visual tool for optimization [51]. Contour plot and 3-D RSM plot is illustrated in fig. 10.

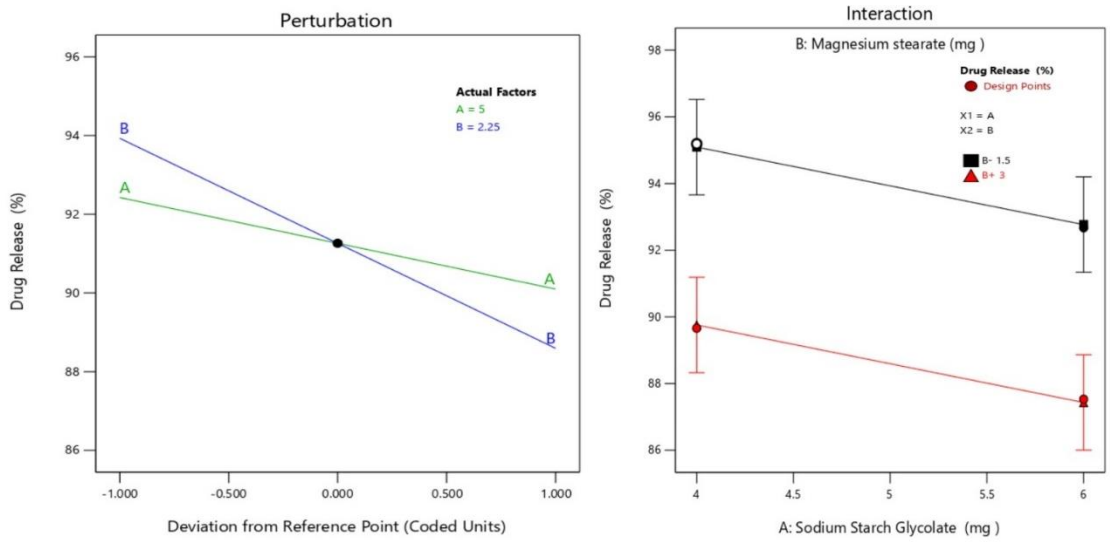

Fig. 9: Interaction plot showing the interaction effect of levels of independent variables on % drug release from the tablet, values of % drug release

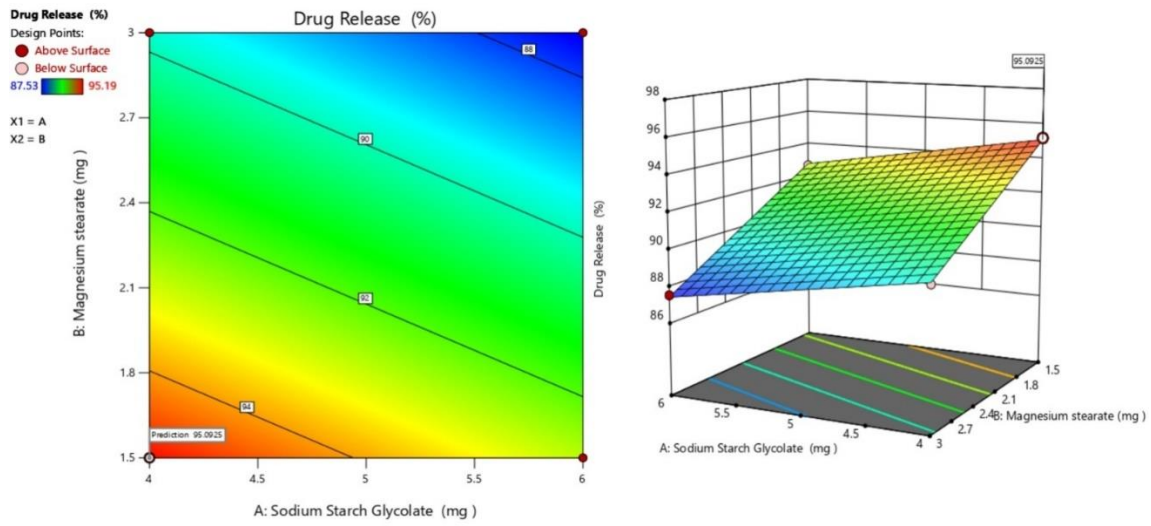

Fig. 10: Contour plot and 3-D RSM plot to depict the combined effect of both the independent variables on the % drug release from the tablet

This response surface plot is mainly used to study the effect of the SSG and MS have at different concentrations on the % drug release. The presence of 3 axes is important to denote the concentration of SSG and MS, and also the % drug release. The colour scale present on the left panel, ranging from blue to red, indicates the low to high % drug release. The plot concludes the optimum action of SSG and MS at lower levels, leading to 95.0925 % drug release. The plain surface of the RSM plot signifies the linearity in the trend, making it reliable to predict the dependent parameter [51].

Desirability analysis

The plots in the fig. 11 are used to depict the impact of concentrations of both SSG and MS on the drug release and desirability of the prepared formulation. The desirability plot shows the most desirable product (0.987) at lower levels of both ingredients; likewise, in the adjacent plot, the highest drug release (95.19 %) predicted is at similar concentrations of SSG and MS. It can be seen that a gradual increase in these concentrations may lead to low drug release making a formulation less desirable. On the basis of desirability analysis F1 batch was considered as an optimized batch with highest drug release. Hence, it can be concluded that the precise quantity of the excipients is of superior importance to formulate an optimized formulation [52, 53].

Evaluation of post-compression parameters of the tablet

The tablets were compressed and evaluated for parameters like variability in weight, hardness and thickness, % friability, time for disintegration and % drug content, results of which are listed in the table below. All parameters that were assessed are found to be well within established limits. All post-compression parameters of tablets are depicted in table 8 [52].

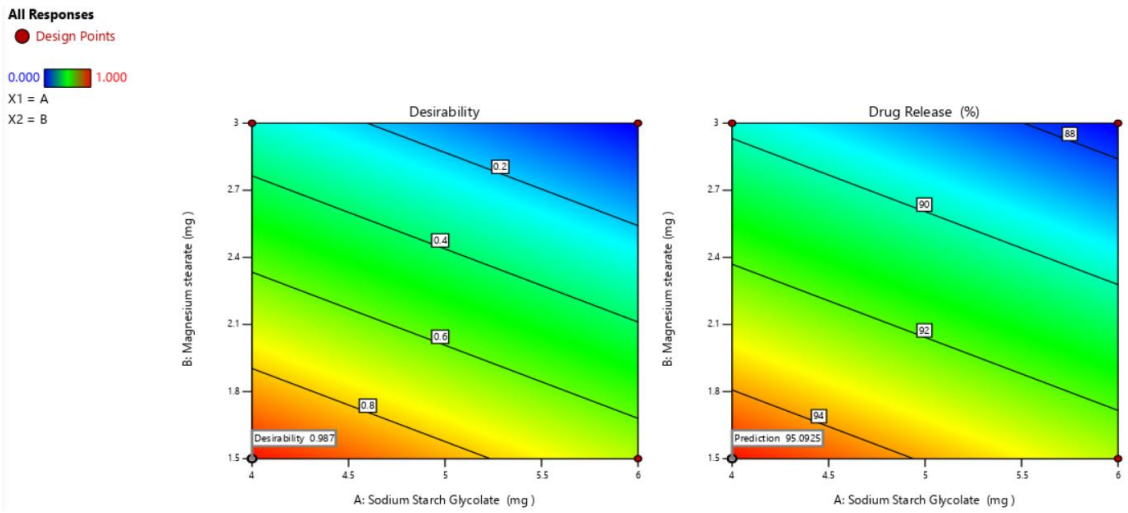

Fig. 11: Plots showing desirability and % drug release at certain concentrations of SSG and MS

Table 8: The table consists of the parameters evaluated post-compression

Parameters	F1	F2	F3	F4	Pure RRB tablet
Weight Variation [mg]	200±1.20	200±1.16	200±1.23	200±1.18	200±1.19
Hardness [kg/cm²]	4.1±0.39	4.2±0.31	4.1±0.27	4.2±0.29	4.2±00.25
Thickness[mm]	4.10±0.60	4.09±0.50	4.12±0.60	4.08±0.40	4.09±0.50
Friability [%]	0.81±0.05	0.76±0.02	0.79±0.03	0.84±0.06	0.72±0.05
Disintegration time [min]	10±1.50	10±1.00	10±1.00	11±1.00	10±1.00
Drug content [%]	99.27±0.67	98.50±0.72	98.64±0.47	99.12±0.29	99.07±0.33

Data presented as mean±SD (n = 3)

Pharmacokinetic analysis

RRB and RRB-CA cocrystals were subjected to comparative pharmacokinetic analysis to estimate the improved systemic availability of drug when administered as a cocrystal. Results of pharmacokinetic study clearly demonstrated the improvement in the parameters like $t_{1/2}$, Cmax, AUC_{0-t} and $AUC_{0-\infty}$. RRB pure drug showed the Cmax 14.3389±1.4116 while RRB-CA cocrystals showed the Cmax23.9644±1.5870. Similarly, AUC_{0-t} and $AUC_{0-\infty}$ was 261.8247±37.2338 and 326.1781±36.2925 for pure RRB while after cocrystallization with CA it was significantly improved. RRB-CA showed the values 406.0891±42.637 and 495.6658±37.78 for AUC_{0-t} and $AUC_{0-\infty}$ respectively. The RRB-CA cocrystal also showed increased half-life t1/2 in comparison to pure RRB. Pure RRB showed the half-life 18.60954±1.81655 while RRB-CA cocrystals showed the half-life of 23.06783±2.9056. Pharmacokinetic study performed using *wistar rat* model clearly demonstrated the comparative improvement in bioavailability of drug after cocrystallization with CA. Fig. 12 illustrate the comparative plasma concentration time profile curve for pure RRB and RRB-CA cocrystals while table 9 illustrates the comparative pharmacokinetic parameters for pure RRB and RRB-CA cocrystals. This improvement in pharmacokinetic parameters of RRB is the result of improved solubility and dissolution after transforming into cocrystals. The new bicomponent crystalline form of RRB has better solubility than existing crystalline form of pure drug [29, 53-56].

Stability study and shelf-life analysis

Comparative accelerated stability analysis performed for 3 mo to reveal the benefits of cocrystallization with stability perspective. RRB-CA cocrystal tablet showed better stability when compared with pure RRB tablet. The formation of stable heterosynthon during cocrystallization results in improved stability in comparison with pure drug. RRB tablets showed shelf life of 15.45 mo while RRB-CA cocrystal tablet showed shelf life of 26.25 mo, which clearly indicates the improved stability after cocrystal formation. Fig. 13a and b illustrate the comparative shelf-life of pure RRB and RRB-CA cocrystals while table 10 illustrates the comparative stability study parameters for RRB and RRB-CA cocrystals [30, 54].

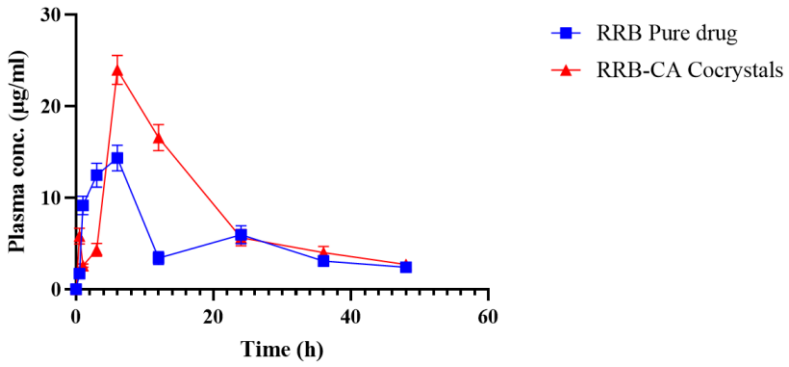

Fig. 12: Comparative plasma concentration time profile curve for pure RRB and RRB-CA cocrystals. Error bars indicate SD values, n=4

Table 9: Pharmacokinetic parameters for pure RRB and RRB-CA cocrystals

S. No.	Pharmacokinetic parameters	RRB Pure drug	RRB-CA Cocrystal
1	$t_{1/2}$*	18.60954±1.81655	23.06783±2.9056
2	Tmax [h]	6	6
3	Cmax* [µg/ml]	14.3389±1.4116	23.9644±1.5870
4	$AUC_{0\text{-}t}$* µg/mlh	261.8247±37.2338	406.0891±42.6370
5	$AUC_{0-\infty}$* µg/mlh	326.1781±36.2925	495.6658±37.7810
6	$AUC_{0\text{-}t/0-\infty}$	0.8008334±0.0254	0.8180757±0.0239
7	$AUMC_{0-\infty}$ µg/mlh^2	9426.3894±478.5224	13909.21667±153.9617
8	$MRT_{0-\infty}$ h	29.03164±1.8030	28.1667±2.1033

Data presented as mean±SD (n = 4). Statistical significance between Pure RRB and RRB–CA cocrystal group was determined by [Student's t-test]; *p<0.05.

Table 10: Comparative shelf-life analysis of pure RRB and RRB-CA cocrystals

Formulation parameter	RRB-CA cocrystal tablet	RRB pure drug tablet
Color	White	White
Odor	No	No
Hardness [kg/cm^2]	4.1±0.27	4.1±0.09
Friability [%]	0.81±0.05	0.82±0.07
Drug content [%]	99.27±0.67	99.07±0.33
Disintegration time[min]	10±1.00	10±1.00
Percent drug release	94.37±1.29	66.49±1.81

Data presented as mean±SD (n = 3)

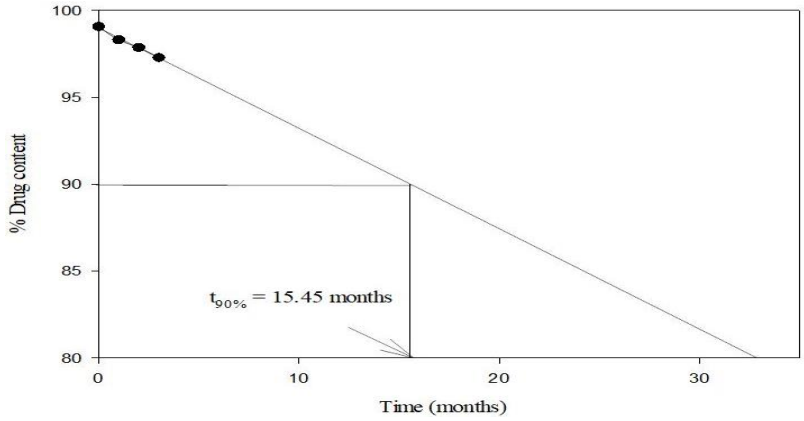

Fig. 13a: Shelf-life analysis of pure RRB

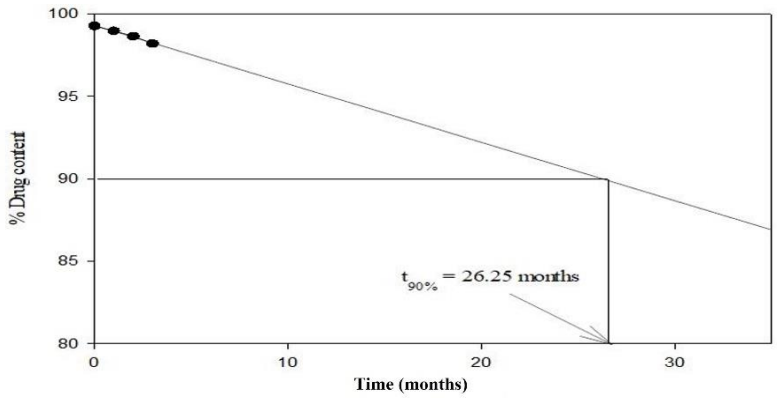

Fig. 13b: Shelf-life analysis of RRB-CA cocrystals

CONCLUSION

Despite of high therapeutic significance of RRB its poor solubility limits its exploration in solid oral formulations. Cocrystallization was found to be a promising approach for enhancing solubility and bioavailability of RRB. Microwave assisted solvent evaporation resulted in robust synthesis of cocrystals. The RRB-CA cocrystal showed highest solubility. Characterizations like FTIR, DSC and XRD

confirmed the formation of cocrystals. Powder dissolution and comparative dissolution of pure RRB and RRB-CA cocrystal tablets revealed the improved dissolution after cocrystallization. Development of cocrystals also resulted in improved flowability of pure RRB it was additionally demonstrated using SeDeM analysis. Comparative pharmacokinetic analysis of RRB pure drug and RRB-CA cocrystals showed improved bioavailability. Pharmacokinetic parameters like Cmax, t1/2 and AUC were significantly improved after cocrystallization. RRB-CA cocrystals showed better stability in comparison with pure RRB. RRB-CA cocrystal tablet showed significantly higher shelf life than pure RRB drug. Crystallographic modification RRB with CA resulted in improved solubility, dissolution, flowability, bioavailability and stability. The cocrystallization of RRB with CA resulted in improved solubility by 5.80 folds while powdered dissolution showed the improvement by 1.65 folds. The results of kinetic study also demonstrated the improvement Cmax by 1.67 folds and AUC by 1.55 folds. Overall, the cocrystallization resulted in improved solubility, dissolution, bioavailability and stability.

FUNDING

No funding was received for this research work.

ABBREVIATIONS

RRB: Rivaroxaban; CA: Citric acid; SeDeM: Sediment Delivery Model; IPP: Parametric Profile Index; IGC: Good Compressibility Index; AUC: Area Under Curve; MRT: mean Residence Time

AUTHORS CONTRIBUTIONS

Deepak Kulkarni: Conceptualization, methodology, investigation, writing. Sanjay Pekamwar: Validation, formal analysis, supervision. Prashant Tanadale: Resources, writing.

CONFLICT OF INTERESTS

Authors declare no conflicts of interest

REFERENCES

1. Alameri MA, Sulaiman DS, Ashour DA, Al-Saati DM. Comparing aspirin enoxaparin and Rivaroxaban post primary total knee replacement: a prospective study from Saudi Arabia. Int J Pharm Pharm Sci. 2021;3(1):31-6. doi: 10.33545/26647222.2021.v3.i1a.66.
2. Mueck W, Stampfuss J, Kubitza D, Becka M. Clinical pharmacokinetic and pharmacodynamic profile of Rivaroxaban. Clin Pharmacokinet. 2014;53(1):1-16. doi: 10.1007/s40262-013-0100-7, PMID 23999929.
3. Savjani KT, Gajjar AK, Savjani JK. Drug solubility: importance and enhancement techniques. ISRN Pharm. 2012;2012:195727. doi: 10.5402/2012/195727, PMID 22830056.
4. Guo M, Sun X, Chen J, Cai T. Pharmaceutical cocrystals: a review of preparations physicochemical properties and applications. Acta Pharm Sin B. 2021;11(8):2537-64. doi: 10.1016/j.apsb.2021.03.030, PMID 34522597.
5. Nangia AK, Desiraju GR. Crystal engineering: an outlook for the future. Angew Chem Int Ed Engl. 2019;58(13):4100-7. doi: 10.1002/anie.201811313, PMID 30488598.
6. Yadav BK, Khursheed A, Cocrystals SRD. A complete review on conventional and novel methods of its formation and its evaluation. Asian J Pharm Clin Res. 2019;12(7):68-74. doi: 10.22159/ajpcr.2019.v12i7.33648.
7. Friscic T, Jones W. Recent advances in understanding the mechanism of cocrystal formation via grinding. Cryst Growth Des. 2009 Mar 4;9(3):1621-37. doi: 10.1021/cg800764n.
8. Thenge RR, Patond VB, Ajmire PV, Barde LN, Mahajan NM, Tekade NP. Preparation and characterization of co-crystals of diacerein. Indonesian J Pharm. 2017;28(1):34. doi: 10.14499/indonesianjpharm28iss1pp34.
9. Kumar Bandaru R, Rout SR, Kenguva G, Gorain B, Alhakamy NA, Kesharwani P. Recent advances in pharmaceutical cocrystals: from bench to market. Front Pharmacol. 2021;12:780582. doi: 10.3389/fphar.2021.780582, PMID 34858194.
10. Raheem Thayyil A, Juturu T, Nayak S, Kamath S. Pharmaceutical co-crystallization: regulatory aspects design characterization and applications. Adv Pharm Bull. 2020;10(2):203-12. doi: 10.34172/apb.2020.024, PMID 32373488.
11. Aher S, Dhumal R, Mahadik K, Paradkar A, York P. Ultrasound assisted cocrystallization from solution (USSC) containing a non-congruently soluble cocrystal component pair: caffeine/maleic acid. Eur J Pharm Sci. 2010;41(5):597-602. doi: 10.1016/j.ejps.2010.08.012, PMID 20801215.
12. Wang Y, Zhang H, Cai L, Xue F, Chen H, Gong J. Polymer-mediated and ultrasound-assisted crystallization of ropivacaine: crystal growth and morphology modulation. Ultrason Sonochem. 2023;97:106475. doi: 10.1016/j.ultsonch.2023.106475, PMID 37321071.
13. Sulistyowaty MI, Setyawan D, Prameswari PP, Susilo RJ, Amrillah T, Zaini E. A comparison study between green synthesis of microwave irradiation and solvent evaporation methods in the formation of p-Methoxycinnamic acid-succinic acid cocrystals. Sci Technol Indones. 2024;9(3):629-36. doi: 10.26554/sti.2024.9.3.629-636.
14. Sakhiya DC, Borkhataria CH. A review on advancement of cocrystallization approach and a brief on screening formulation and characterization of the same. Heliyon. 2024 Apr 15;10(7):e29057. doi: 10.1016/j.heliyon.2024.e29057, PMID 38601657.
15. Ahuja D, Ramisetty KA, Sumanth PK, Crowley CM, Lusi M, Rasmuson AC. Microwave assisted slurry conversion crystallization for manufacturing of new co-crystals of sulfamethazine and sulfamerazine. Cryst Eng Comm. 2020;22(8):1381-94. doi: 10.1039/C9CE01886G.
16. Ionita S, Patraşcu M, Soare EM, Lincu D, Atkinson I, Rusu A. Rapid synthesis and evaluation of resveratrol-piperazine cocrystals by ultrasound and microwave methods. Pharm Res. 2024;41(9):1843-53. doi: 10.1007/s11095-024-03758-3, PMID 39112777.
17. Machado TC, Kuminek G, Cardoso SG, Rodriguez Hornedo N. The role of pH and dose/solubility ratio on cocrystal dissolution drug supersaturation and precipitation. Eur J Pharm Sci. 2020;152:105422. doi: 10.1016/j.ejps.2020.105422, PMID 32531350.
18. Andres A, Roses M, Rafols C, Bosch E, Espinosa S, Segarra V. Setup and validation of shake-flask procedures for the determination of partition coefficients (logD) from low drug amounts. Eur J Pharm Sci. 2015;76:181-91. doi: 10.1016/j.ejps.2015.05.008, PMID 25968358.
19. Panzade P, Shendarkar G, Kulkarni D, Shelke S. Solid state characterization and dissolution enhancement of nevirapine cocrystals. Adv Pharm Bull. 2021;11(4):772-6. doi: 10.34172/apb.2021.087, PMID 34888225.
20. Pekamwar SS, Kulkarni DA. Nanded-431 606, Maharashtra India. Development and evaluation of bicomponent cocrystals of aceclofenac for efficient drug delivery with enhanced solubility and improved dissolution. Ind Dru. 2021;58(8):54-60. doi: 10.53879/id.58.08.12691.
21. Kulkarni D. Accidental formation of eutectics during crystal engineering of lamotrigine with solubility advantage and drug release efficiency. Asian J Pharm. 2021;15(1):60-7. doi: 10.22377/ajp.v15i1.3960.
22. Rao MR, Patil M, Bagwan B, Patil P, Bhaleghare I. Physico-mechanistic studies on effect of spray drying and corrective excipients on direct compressibility of nanosponges by SeDeM analysis. Drug Dev Ind Pharm. 2025;51(8):1-13. doi: 10.1080/03639045.2025.2522854, PMID 40548725.
23. Sune Negre JM, Garcia E, Perez P, Aguilar Diaz JE, Roig M, Fuster R. SeDeM diagram: a new expert system for the formulation of drugs in solid form. In: Vizureanu P, editor. Expert systems for human materials and automation. InTech; 2011. p. 17-34. doi: 10.5772/16540.
24. Panzade P, Shendarkar G, Shaikh S, Balmukund Rathi P. Pharmaceutical cocrystal of piroxicam: design formulation and evaluation. Adv Pharm Bull. 2017;7(3):399-408. doi: 10.15171/apb.2017.048, PMID 29071222.
25. Gadade DD, Kulkarni D, Rathi P, Pekamwar SS, Joshi S. Solubility enhancement of lornoxicam by crystal engineering. Indian J Pharm Sci. 2017;79(2):277-86. doi: 10.4172/pharmaceutical-sciences.1000226.
26. Gaikwad SS, Kshirsagar SJ. Application of tablet in tablet technique to design and characterize immediate and modified release tablets of timolol maleate. Heliyon. 2024;10(3):e25820. doi: 10.1016/j.heliyon.2024.e25820, PMID 38356537.

27. Ozon EA, Mati E, Karampelas O, Anuta V, Sarbu I, Musuc AM. The development of an innovative method to improve the dissolution performance of Rivaroxaban. Heliyon. 2024;10(12):e33162. doi: 10.1016/j.heliyon.2024.e33162, PMID 39021978.
28. Meng Y, Tan F, Yao J, Cui Y, Feng Y, Li Z. Preparation characterization and pharmacokinetics of Rivaroxaban cocrystals with enhanced *in vitro* and *in vivo* properties in beagle dogs. Int J Pharm X. 2022;4:100119. doi: 10.1016/j.ijpx.2022.100119, PMID 35663355.
29. Kakulade S, Kulkarni D, Moravkar K, Zambad S, Tekade A, Chalikwar S. Development characterization and pharmacokinetic evaluation of selegiline HCl loaded cubosomal thermoreversible mucoadhesive gel for nose to brain delivery. J Drug Deliv Sci Technol. 2024;100:106111. doi: 10.1016/j.jddst.2024.106111.
30. Aitipamula S, Wong AB, Chow PS, Tan RB. Pharmaceutical cocrystals of ethenzamide: structural solubility and dissolution studies. CrystEngComm. 2012 Nov 12;14(24):8515-24. doi: 10.1039/c2ce26325d.
31. Desiraju GR. Supramolecular synthons in crystal engineering a new organic synthesis. Angew Chem Int Ed Engl. 1995;34(21):2311-27. doi: 10.1002/anie.199523111.
32. Huang S, Cheemarla VK, Tiana D, Lawrence SE. Experimental and theoretical investigation of hydrogen-bonding interactions in cocrystals of sulfaguanidine. Cryst Growth Des. 2023 Apr 5;23(4):2306-20. doi: 10.1021/acs.cgd.2c01337, PMID 37038403.
33. Shiraki K, Takata N, Takano R, Hayashi Y, Terada K. Dissolution improvement and the mechanism of the improvement from cocrystallization of poorly water-soluble compounds. Pharm Res. 2008 Nov 1;25(11):2581-92. doi: 10.1007/s11095-008-9676-2, PMID 18651208.
34. Nawatila R, W AN, Siswodihardjo S, Setyawan D. Preparation of acyclovir-nicotinamide cocrystal by solvent evaporation technique with variation of solvent. Asian J Pharm Clin Res. 2017;10(3):283-7. doi: 10.22159/ajpcr.2017.v10i3.16149.
35. Sanphui P, Devi VK, Clara D, Malviya N, Ganguly S, Desiraju GR. Cocrystals of hydrochlorothiazide: solubility and diffusion/permeability enhancements through drug–coformer interactions. Mol Pharm. 2015;12(5):1615-22. doi: 10.1021/acs.molpharmaceut.5b00020, PMID 25800383.
36. Nadendla RR, Satynarayana J, Burri JK. Rivaroxaban: compatibilty with pharmaceutical excipients using DSC and FTIR spectrophotometry. J Pharm Res Int. 2022;34(12A):43-50. doi: 10.9734/jpri/2022/v34i12A35554.
37. Bichara LC, Lanus HE, Brandan SA. Stabilities of aqueous solutions of sucrose containing ascorbic and citric acids by using FTIR spectroscopy and physicochemical studies. J Mol Liq. 2014;200:448-59. doi: 10.1016/j.molliq.2014.10.038.
38. Zhai L, Zhang Z, Guo L, Zhu Z, Hu C, Zhang G. Synthesis characterization and properties of Rivaroxaban new crystalline forms. Cryst Res Technol. 2021;56(9):2000243. doi: 10.1002/crat.202000243.
39. Lu Q, Zografi G. Properties of citric acid at the glass transition. J Pharm Sci. 1997;86(12):1374-8. doi: 10.1021/js970157y, PMID 9423149.
40. Shaligram PS, George CP, Sharma H, Mahadik KR, Patil S, Vanka K. Rivaroxaban eutectics with improved solubility dissolution rates bioavailability and stability. CrystEngComm. 2023;25(22):3253-63. doi: 10.1039/D3CE00261F.
41. Singh KA, Pathak LC, Roy SK. Effect of citric acid on the synthesis of nano-crystalline yttria stabilized zirconia powders by nitrate–citrate process. Ceram Int. 2007;33(8):1463-8. doi: 10.1016/j.ceramint.2006.05.021.
42. Scholtz JC, Steenekamp JH, Hamman JH, Tiedt LR. The SeDeM expert diagram system: its performance and predictability in direct compressible formulations containing novel excipients and different types of active ingredients. Powder Technol. 2017;312:222-36. doi: 10.1016/j.powtec.2017.02.019.
43. Panzade P, Shendarkar G. Superior solubility and dissolution of zaltoprofen via pharmaceutical cocrystals. Turk J Pharm Sci. 2019;16(3):310-6. doi: 10.4274/tjps.galenos.2018.15013, PMID 32454729.
44. Shiekmydeen J, Tanisha SS, Sharma S, Chakraborty K, Kannaiyan DC, Khan NA. Optimization of wet granulation process for manufacturing Rivaroxban generic immediate-release tablets using PBPK modeling and simulations. In Silico Pharmacol. 2024;12(2):77. doi: 10.1007/s40203-024-00249-6, PMID 39184229.
45. Panzade P, Shendarkar G. Design and preparation of zaltoprofen-nicotinamide pharmaceutical cocrystals via liquid assisted grinding method. Indian J Pharm Educ Res. 2019;53(4s):s563-70. doi: 10.5530/ijper.53.4s.151.
46. Fernandes GJ, Rathnanand M. Formulation optimization for gastroretentive drug delivery system of carvedilol cocrystals using design of experiment. J Pharm Innov. 2020;15(3):455-66. doi: 10.1007/s12247-019-09393-5.
47. Daniel C. Use of half-normal plots in interpreting factorial two-level experiments. Technometrics. 1959;1(4):311-41. doi: 10.1080/00401706.1959.10489866.
48. Modi C, Bharadia P. Pareto chart-enabled screening of influential factors in designing transfersomes. Sep Sci Plus. 2023;6(1):2200082. doi: 10.1002/sscp.202200082.
49. Eaton J, Deng G, Hauck WW, Brown W, Manning RG, Wahab S. Perturbation study of dissolution apparatus variables a design of experiment approach. Diss Technol. 2007;14(1):20-6. doi: 10.14227/DT140107P20.
50. Campisi B, Chicco D, Vojnovic D, Phan-Tan-Luu R. Experimental design for a pharmaceutical formulation: optimisation and robustness1. J Pharm Biomed Anal. 1998;18(1-2):57-65. doi: 10.1016/S0731-7085(98)00175-7, PMID 9863943.
51. Singh Chundawat LS, Sharma V. Formulation evaluation and optimization of orodispersible tablets of pantoprazole sodium by the using of different superdisintegrants. Asian J Pharm Clin Res. 2018;11(5):84-9. doi: 10.22159/ajpcr.2018.v11i5.24595.
52. Devi S, Kumar A, Kapoor A, Verma V, Yadav S, Bhatia M. Ketoprofen–FA co-crystal: *in vitro* and *in vivo* investigation for the solubility enhancement of drug by design of expert. AAPS PharmSciTech. 2022;23(4):101. doi: 10.1208/s12249-022-02253-5, PMID 35348937.
53. Kasar HA, Dev A, Dhal S. Formulation and evaluation of lidocaine hydrochloride chewable tablet. Asian J Pharm Clin Res. 2018;11(11):190-4. doi: 10.22159/ajpcr.2018.v11i11.27057.
54. Latif S, Abbas N, Hussain A, Arshad MS, Bukhari NI, Afzal H. Development of paracetamol-caffeine co-crystals to improve compressional formulation and *in vivo* performance. Drug Dev Ind Pharm. 2018;44(7):1099-108. doi: 10.1080/03639045.2018.1435687, PMID 29385849.
55. Ren S, Jiao L, Yang S, Zhang L, Song J, Yu H. A novel co-crystal of bexarotene and ligustrazine improves pharmacokinetics and tissue distribution of bexarotene in SD rats. Pharmaceutics. 2020;12(10):906. doi: 10.3390/pharmaceutics12100906, PMID 32977470.
56. Hrinova E, Skorepova E, Cerna I, Kralovicova J, Kozlik P, Kiizek T. Explaining dissolution properties of Rivaroxaban cocrystals. Int J Pharm. 2022;622:121854. doi: 10.1016/j.ijpharm.2022.121854, PMID 35623488.